applied sciences

MDPI

Article

Biomechanical Effect of 3D-Printed Foot Orthoses in Patients with Knee Osteoarthritis

Kuang-Wei Lin [1], Li-Wei Chou [1], Yi-Tien Su [2], Shun-Hwa Wei [1] and Chen-Shen Chen [1,*]

[1] Department of Physical Therapy and Assistive Technology, National Yang Ming Chiao Tung University, Taipei 112, Taiwan; wade1112@gm.ym.edu.tw (K.-W.L.); lwchou@ym.edu.tw (L.-W.C.); shunhwa@ym.edu.tw (S.-H.W.)
[2] Department of Rehabilitation, Far Eastern Memorial Hospital, Taipei 220, Taiwan; yitiensu@gmail.com
* Correspondence: cschen@ym.edu.tw; Tel.: +886-2-2826-7353

Abstract: Lateral wedges are a common conservative treatment for medial knee osteoarthritis (OA). However, use of lateral wedges might increase the ankle eversion moment. To minimize the risk of ankle symptoms, lateral wedges with custom arch support are suggested. However, the manufacturing process of a custom foot orthosis (FO) is complicated, labor-intensive, and time-consuming. The technology of 3D printing is an ideal method for mass customization. Therefore, the purpose of this study was to develop custom FOs using 3D-printing techniques and to evaluate the effects of 3D-printed FOs in patients with knee OA. Fifteen patients with medial knee OA were enrolled into this study. Kinematic and kinetic data were collected during walking by using an optical motion capture system. A paired-sample *t*-test was conducted to compare biomechanical variables under two conditions: walking in standard shoes (Shoe) and walking in shoes embedded with 3D-printed FOs (Shoe + FO). The results show that the first and second peak knee adduction moments were significantly reduced by 4.08% and 9.09% under the Shoe + FO condition. The FOs alter the biomechanical environment in a way that reduces the variables used to infer abnormal loads at the knee and ankle that could result in painful symptoms.

Keywords: knee adduction moment; center of pressure; foot orthoses; 3D printing; 3D scan

Citation: Lin, K.-W.; Chou, L.-W.; Su, Y.-T.; Wei, S.-H.; Chen, C.-S. Biomechanical Effect of 3D-Printed Foot Orthoses in Patients with Knee Osteoarthritis. *Appl. Sci.* **2021**, *11*, 4200. https://doi.org/10.3390/app11094200

Academic Editor: Hanatsu Nagano

Received: 25 March 2021
Accepted: 3 May 2021
Published: 5 May 2021

1. Introduction

Knee osteoarthritis (OA) is one of the most common musculoskeletal diseases in elderly people. The global age-standardized prevalence of symptomatic knee OA is 3.8% [1]. It affects 8.1% of adults in China and is more common in women (10.3%) than in men (5.7%) [2]. The medial knee compartment is the site most commonly affected by OA [3].

The primary goal of many treatment approaches is to reduce the medial knee compartment contact force. However, it is very difficult to directly measure the medial knee compartment contact force in vivo. The external knee adduction moment (KAM) is often used as a surrogate measure of the medial knee compartment contact force; the KAM increases the contact force by rotating the tibia medially with respect to the femur in the frontal plane [4,5]. The peak knee flexion moment (KFM) is another important predictor of peak loading. In a linear regression model, the combination of the peak KAM and KFM provides a more accurate estimate of the peak medial knee compartment contact force than the peak KAM alone [6]. Both the KAM and KFM should be employed when investigating the knee joint loading indirectly. To reduce the KAM, nonsurgical treatment options include the use of a cane [7], the use of knee braces [8], gait modification [9], and the use of lateral wedges [10].

Lateral wedges are a common conservative treatment for medial knee OA. They shift the center of pressure (COP) laterally to decrease the adduction moment arm at the knee [10]. Previous studies have shown that lateral wedges with an inclination of 5° or 6° significantly reduced the peak KAM by 4–6% during level walking compared to walking without a wedge [10–12]. However, the lateral shift in the COP also increases the ankle eversion moment (AEM) [13]. This might have implications for patients with knee OA who have acute ankle sprains or chronic ankle instability [14]. Moreover, the use of lateral wedges has been indicated to increase eversion of ankle joint [10] and stride width [15] during walking. An increased stride width increases mediolateral ground reaction force (GRF), that might influence the reduction of KAM. To minimize the risk of ankle symptoms in patients with medial knee OA, lateral wedges with custom arch support are suggested [16]. A previous study showed that when patients with medial knee OA wore lateral wedges, individual biomechanical responses, such as the frontal plane moment arm of the GRF at the knee and the peak KAM, ranged from decreases of approximately 25% to increases of over 20% [17]. A possible explanation for this variability in the responses is the foot posture. The prescription of orthotic devices should be patient-specific. This is because various levels of malalignments likely require different FO designs. However, the manufacturing process of a custom foot orthosis (FO) is complicated, labor-intensive, and time-consuming.

In the conventional subtractive manufacturing process, materials are removed from a larger piece to form the FO. In contrast to subtractive manufacturing, additive manufacturing or three-dimensional (3D) printing processes fabricate objects by adding material layer by layer, and this may be a useful alternative to subtractive manufacturing methodologies. The technology of 3D printing is an ideal method for mass customization, because it has the potential for fabricating customized FOs at relatively low prices and eliminates much of the labor [18]. Moreover, custom FOs fabricated by combining 3D printing with 3D surface scanning and computer-aided design can produce positive biomechanical effects [19].

Therefore, the purpose of this study was to develop custom FOs using 3D printing techniques and to evaluate the changes of COP path, and knee and ankle joint moments in patients wearing the 3D-printed FOs during level walking. This study hypothesized that the 3D-printed FOs would decrease the peak KAM, KFM, AEM, and ankle inversion moment (AIM), and shift the COP path laterally.

2. Materials and Methods

This single-group, pretest–posttest trial was conducted to evaluate the efficacy of using 3D-printed FOs as the intervention in patients with medial knee OA. The present study focused on the biomechanical effects of 3D-printed FOs and analyzed data for the participants who wore and did not wear the 3D-printed FOs. All participants completed all orthotic tests on the same day. The study was approved by the regional ethics committee and conducted according to the Declaration of Helsinki (protocol code: YM106118E, 31 March 2018).

Sample size was based upon our previous work [20]. The result indicated that a sample size of fourteen would be enough to detect a 5% difference in peak KAM, with a statistical power of 80% and a 5% level of significance. Fifteen patients (2 males and 13 females; age, 60.13 $\pm$ 6.10 years; height, 1.59 $\pm$ 0.05 m; and weight, 70.65 $\pm$ 14.16 kg) with radiographically diagnosed medial knee OA (Kellgren–Lawrence grade I or II) were recruited for this study. All participants underwent physical examination and met the American College of Rheumatology criteria [21]. Predominant lateral or patellofemoral OA, or a history of planned hip or knee replacement, hip or ankle arthritis, rheumatoid arthritis, and inability to walk without a cane or walker were the exclusion criteria for this study.

Figure 1 presents the procedure of 3D-printed FO manufacturing. To design and fabricate 3D-printed FOs, non-weight-bearing 3D surface scans of both feet were taken with the foot and ankle in the subtalar neutral position by using the EinScan-Pro handheld 3D scanner (Shining 3D Tech Co., Ltd., Hangzhou, China). The generated 3D foot model was exported as an STL file. The 3D foot model was smoothed and edited using Meshmixer software (Autodesk Inc., San Rafael, CA, USA). In the software program, we used the plantar surface as the shell of FO (Figure 2), extracted the shell of FO, and extruded it to produce a 2.5-mm-thick FO.

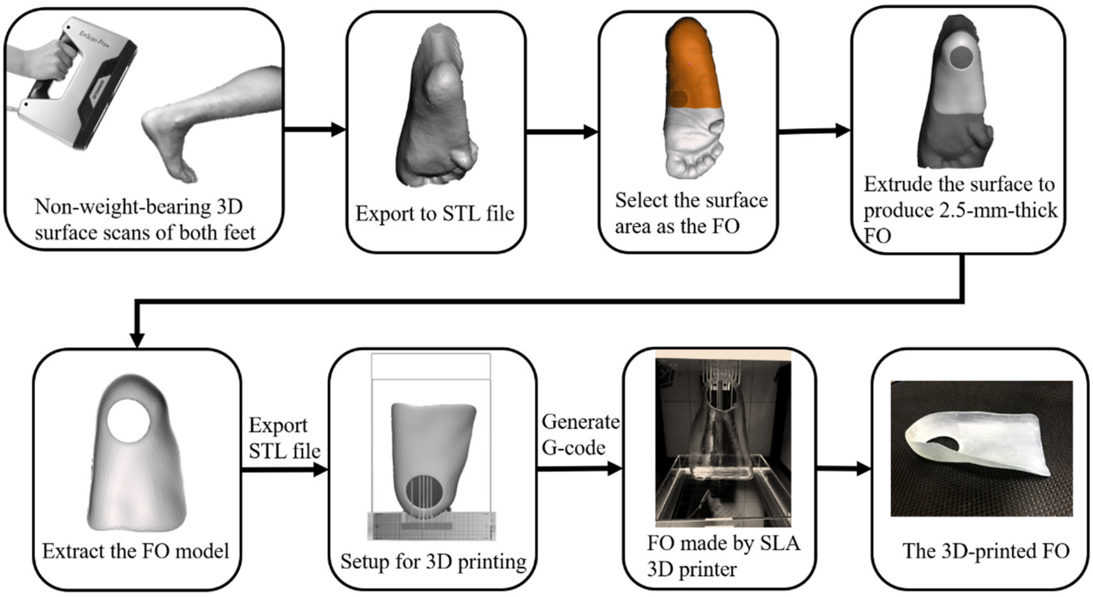

Figure 1. Procedure of 3D printing for foot orthoses.

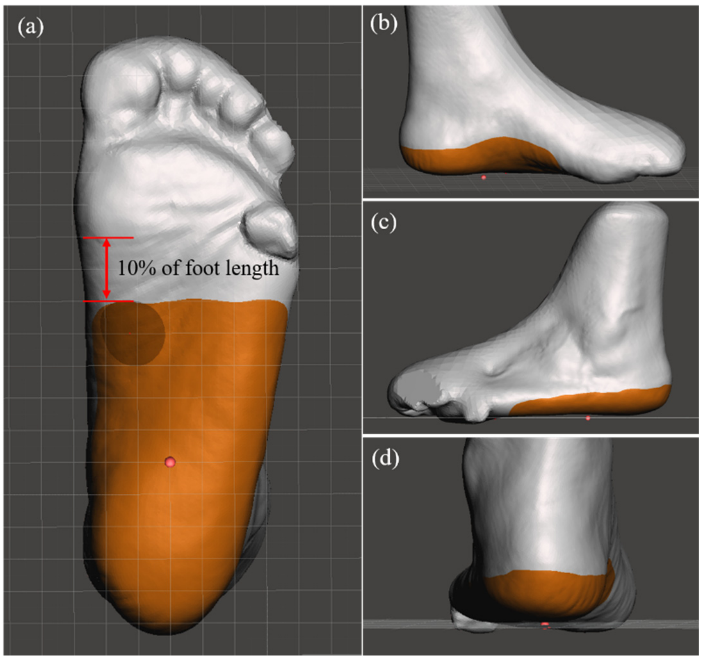

Figure 2. (**a**) The shell ends near the metatarsal heads. The distance between the shell end and the first metatarsal head is approximately 10% of foot length. (**b**) Medial shell ends near navicular tuberosity. (**c**) Lateral and (**d**) rear edges of shell.

All FOs were manufactured in photosensitive polymer resins with material properties conducive to producing semi-rigid FOs (tensile strength, 45 MPa; Young's modulus, 1500 MPa; elongation at break, 30%; shore hardness, 84 D) by using a stereolithography (SLA) 3D printer (Moai; Peopoly, CA, USA). The SLA 3D printer uses a laser to cure photosensitive polymer resins into 3D objects. Figure 3 demonstrates the rear and medial view of the 3D-printed FO. The bottom of the 3D-printed FO is not a flat surface. Because of the geometric shapes of the 3D-printed FO, it may provide not only medial support but also lateral support.

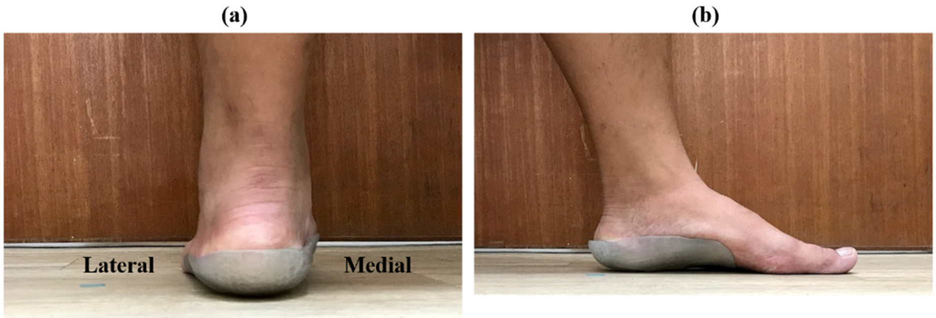

Figure 3. (**a**) Rear view and (**b**) medial view of the foot orthosis.

Reflective marker placement was described in the previous work [20]. Moreover, two clusters of three noncollinear markers on rigid plates were mounted on the skin of the thigh and shank (Figure 4). Prior to data collection, the participants were allowed to become familiar with the two experimental conditions: walking in standard shoes (Shoe) and walking in standard shoes embedded with 3D-printed FOs (Shoe + FO). In this study, we used kung fu shoes as the standard shoes. The kung fu shoe was made with minimal lining, a soft toe box, and a flat hard plastic sole. The participants completed five trials of level walking at the self-selected speed under each condition. The order of the two experimental conditions was randomized for each participant. An eight-camera motion analysis system operating at 100 Hz (Vicon MX T20; Vicon Motion Systems Ltd., Oxford, UK) and three force plates operating at 1000 Hz (AMTI, Advanced Mechanical Technology Inc., Watertown, MA, USA) were used to measure the kinematic data and GRF.

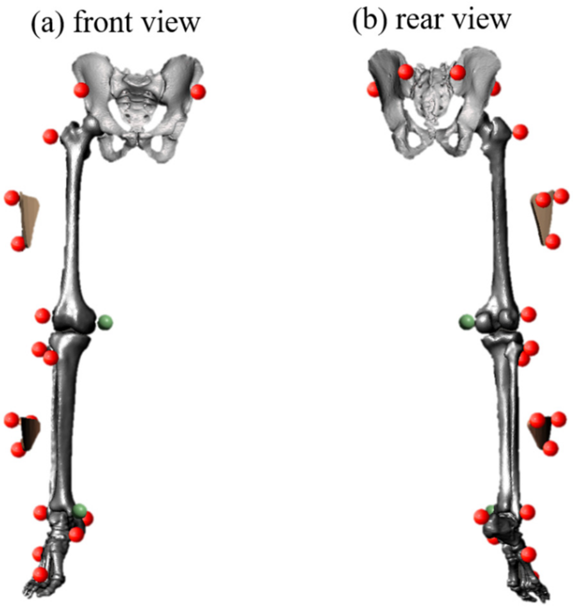

Figure 4. (**a**) Frontal view and (**b**) rear view of marker placement. The green markers would be removed during dynamic trials.

All data were processed using a custom-written software program (MATLAB 2018a; MathWorks Inc., Natick, MA, USA). The marker data were filtered using a fourth-order zero-lag Butterworth 8-Hz low-pass filter. Static reference measurement was conducted to measure the locations of the markers (medial femoral epicondyle and medial malleolus) with respect to the cluster markers and to define neutral joint orientations. These two markers were removed for the dynamic trials. The joint angles were obtained following a *z*-*x*-*y* Cardan rotation sequence. The knee and ankle joint centers were determined based on the midpoint between the medial and lateral markers. With the measured GRF and kinematic data, inverse dynamics using Newton–Euler equations of motion were used to calculate the joint moments of lower limbs, as shown in Equation (1). Moments are reported herein as external moments. The path of the COP was computed based on the COP position of the global coordinate system relative to the position of the second metatarsal and heel markers [22]. The midline of the foot was defined as the vector constructed by the heel and second metatarsal markers. The KAM during level walking was regarded as the primary outcome measure. The KFM, ankle joint moment, COP path, and walking speed were regarded as the secondary outcomes.

$$\vec{M}_P = \boldsymbol{R}\dot{\vec{H}} - \vec{M}_D - \vec{r}_D \times \vec{R}_D - \vec{r}_P \times \vec{R}_P \quad (1)$$

In Equation (1), $\vec{M}_P$ and $\vec{M}_D$ are the proximal and distal joint moments, $\boldsymbol{R}$ is the rotation matrix, $\dot{\vec{H}}$ is the differential angular momentum, $\vec{r}_D$ and $\vec{r}_P$ are the vectors from center of mass to distal and proximal joint centers, $\vec{R}_D$ and $\vec{R}_P$ are the distal and proximal reaction forces.

Statistical analyses were performed using IBM SPSS Statistics version 20.0 software (IBM, Armonk, NY, USA). Prior to statistical analysis, the data were checked for normality through the Shapiro–Wilk test. Normally distributed results were obtained for all variables in the analysis. A paired-sample *t*-test was used to compare the walking speed and peak joint moments under the Shoe and Shoe + FO conditions. The statistical significance level was set at 0.05.

3. Results

3.1. Walking Speed

No significant differences in the walking speed were observed between the two experimental conditions (Table 1).

Table 1. Comparison of the walking speed and biomechanical variables between two conditions: wearing standard shoes (Shoe) and wearing shoes embedded with 3D-printed FO (Shoe + FO).

Variable	Shoe (Mean ± SD)	Shoe + FO (Mean ± SD)	p Value	Effect Size
Walking speed (m/s)	0.977 ± 0.163	0.925 ± 0.146	0.060	0.34
COP at peak KAM (mm)	7.289 ± 3.641	9.998 ± 4.054	0.001 *	0.70
1st peak KAM (N·m·BW^{-1}·LL^{-1})	0.049 ± 0.018	0.047 ± 0.019	0.042 *	0.11
2nd peak KAM (N·m·BW^{-1}·LL^{-1})	0.044 ± 0.017	0.040 ± 0.018	0.004 *	0.23
Peak KFM (N·m·BW^{-1}·LL^{-1})	0.036 ± 0.022	0.034 ± 0.019	0.464	0.10
Peak AEM (N·m·BW^{-1}·LL^{-1})	−0.009 ± 0.005	−0.010 ± 0.006	0.411	0.18
Peak AIM (N·m·BW^{-1}·LL^{-1})	0.009 ± 0.008	0.007 ± 0.008	0.033 *	0.25

* Significantly different between the two conditions. (COP: center of pressure, KAM: knee adduction moment, KFM: knee flexion moment, AEM: ankle eversion moment, AIM: ankle inversion moment, BW: body weight, LL: leg length).

3.2. Center of Pressure

Figure 5 reveals the average path of COP under the two conditions. For the Shoe + FO condition, the COP was more lateral than that under the Shoe condition from the 10% to 90% of the stance phase. Under Shoe + FO, the COP at the peak KAM significantly shifted laterally by 2.71 mm on average compared with that under the Shoe condition (Table 1).

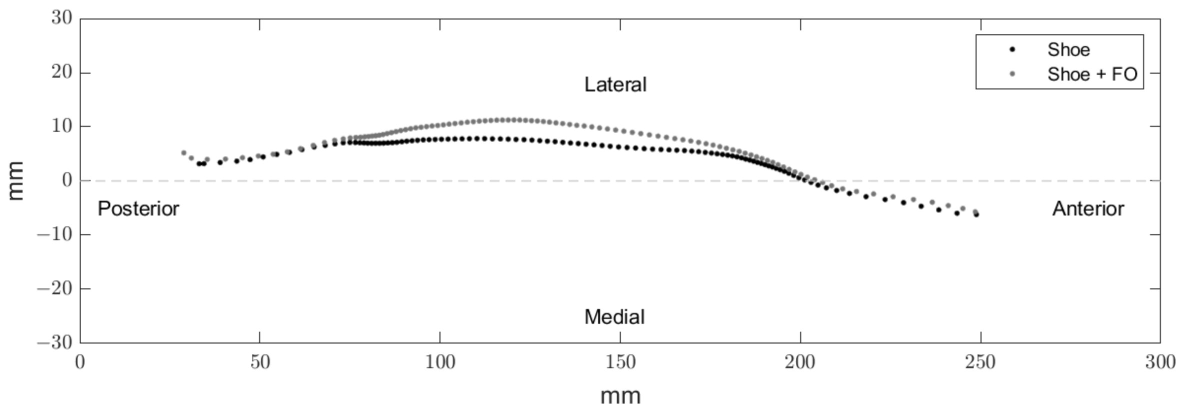

Figure 5. Average center-of-pressure path of two different experimental conditions during level walking. The dashed line represents the long axis of the foot.

3.3. Joint Moments

The KAM presented a two-peak pattern during the stance phase under both experimental conditions (Figure 6a). Therefore, the stance phase in this study was divided into weight-bearing (0–50%) and propulsion phases (51–100%). The first peak in the weight-bearing phase and the second peak in the propulsion phase were extracted. The peak KFM was extracted from the weight-bearing phase (Figure 6b). Moreover, the peak AEM and AIM were extracted from the entire stance phase (Figure 6c).

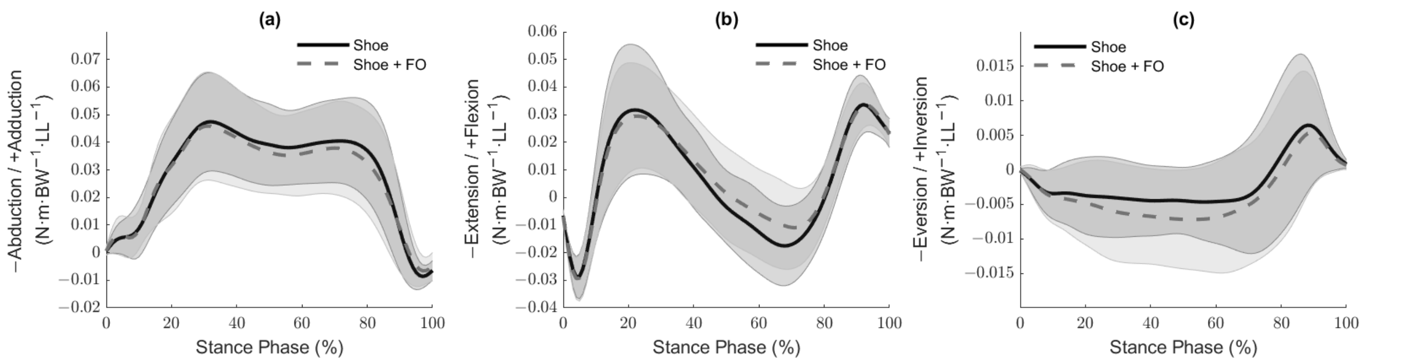

Figure 6. External joint moments for (**a**) knee frontal, (**b**) knee sagittal, and (**c**) ankle frontal plane. The black, solid line represents the Shoe condition; the gray dashed line represents the Shoe + FO condition.

The results showed the first and second peak KAM were significantly reduced by 4.08% and 9.09%, respectively, on average under the Shoe + FO condition (Table 1). Although the peak KFM on average was reduced under the Shoe + FO condition, the peak KFM did not differ significantly under the two experimental conditions. Moreover, the peak AIM was significantly reduced by 22.22% on average under the Shoe + FO condition. The greater AEM was observed under the Shoe + FO condition; however, no significant difference was observed between the two experimental conditions.

4. Discussion

The primary aim of this study was to investigate the biomechanical alterations in knee and ankle joint kinetics as a result of personalized 3D-printed FOs. The key findings of this study are that under the Shoe + FO condition, the first and second peak KAMs and the peak AIM decreased; but no significant differences were observed in the KFM and AEM. Besides this, the mean value and standard deviation can be used to calculate the effect size. The Shoe + FO condition exhibited a more lateral shifting compared to the Shoe condition, with a medium-to-large effect size.

Changes in the joint moment are due to the magnitude of the GRF, the lever arm distance between the GRF vector and the joint center, or both [23]. Moreover, the magnitude of the GRF is associated with walking speed [24]. In the present study, no significant differences were observed in the walking speed between the two experimental conditions. Therefore, we can assume that the alternations of the joint moments by the 3D-printed FOs were due to changes in the COP path.

The reduction of the KAM was caused by the lateral shifting of the COP, decreasing the moment arm around the knee joint, when using lateral wedges [10]. Under the Shoe + FO condition, a similar pattern of COP trajectory was observed; therefore, the first and second peak KAMs decreased. This result is in agreement with those of previous studies [12,25]; there were significant changes in the reduction of the peak KAM in response to lateral wedges with arch support. However, the 3D-printed FOs in this study were used without any additional lateral posting wedges. The 3D-printed FOs may provide lateral support, due to the geometric shapes. A similar design of FO was presented in our previous study [20]. The FOs reduced the moments at ankle joints in individuals with flexible flatfoot, but no significant difference was observed in the knee and hip joint moments. The reason for this difference might be that the individuals with flexible flatfoot do not have severe problems of malalignment of the lower limbs. Therefore, we believe that the 3D-printed FO maintained the foot posture in the neutral position as much as possible during walking, which changed the COP path and contributed to correcting the malalignment of lower limbs.

The use of lateral wedges increased the AEM and ankle eversion angle. However, the lateral wedge with an arch support tended to reduce the ankle eversion angle, while keeping the AEM equal to the level of lateral wedge without an arch support [26]. Although the ankle eversion angle is not reported in this study, the peak AEM was not affected by the 3D-printed FOs. To correct the malalignment of lower limbs, the 3D-printed FOs were semi-rigid and manufactured in photosensitive polymer resins by a 3D printer. In addition, the FOs were made based on the 3D scanning method, which captured the patients' foot shape in the subtalar neutral position. The joint moments in the frontal plane are primarily responsible for the dynamic stability of the lower extremities [27]. Using 3D-printed FOs as interventions affected ankle moments that were highly associated with dynamic stability by decreasing the AIM. The 3D-printed FOs did not influence the AEM but decreased the AIM and KAM; therefore, it may be reasonable to assume that the 3D-printed FO allowed the patients with knee OA to walk in a more natural manner.

To investigate the dynamic loading of the knee, the KFM should be considered [6]. However, 3D-printed FOs did not significantly affect the KFM in the present study. Trepczynski et al. [28] used instrumented prostheses to record in vivo tibiofemoral contact forces during several activities. They suggested that the KFM considerably contributed to medial knee contact force only during the activities with high knee flexion, such as sit-to-stand-to-sit, squatting, and stair negotiation. In this study, the patients with knee OA were only asked to walk on a level floor; therefore, most of the alteration of medial knee loading can be explained by the KAM. Moreover, both the first and second peak KAMs were reduced significantly by the experimental interventions in this study. The magnitude of the peak KAM is associated with increased disease severity [29], pain [30], rate of progression [31], and cartilage thickness [32]. Thus, 3D-printed FOs can still produce positive immediate biomechanical effects in patients with knee OA.

The calculations of knee joint moment need a good accuracy for capturing lower limb kinematics and calculating joint centers. A previous study investigated the reliability of five different knee-joint-center estimation techniques (femoral epicondyle, femoral condyle, tibial ridges, plug-in-gait model, and functional technique) [33]. The knee joint center for the femoral epicondyle, femoral condyle, and tibial ridges configurations were determined by the midpoint between the medial and lateral femoral epicondyles, femoral condyle, and tibial ridge markers. However, they found that no significant differences in the peak knee adduction between femoral epicondyle and functional configurations. In addition, knee joint moments were associated with the highest reliability in all three planes for the femoral epicondyle configuration. Therefore, the femoral epicondyles technique can be used to estimate the knee joint center in this study.

The design and manufacture of custom 3D-printed FOs consist of three main steps: foot geometry capture, FO design, and FO manufacture. The time taken for both the 3D scan of feet and the FO geometric design was approximately 6 and 10 min, respectively. The print time of each FO was approximately 6 h. Nevertheless, the traditional fabrication process for FO normally takes from 7 to 14 days, depending on the manufacturer. The conventional method of custom-making an FO is to take a plaster cast of the foot, but the use of plaster casts may have some reliability problems [34]. By contrast, the 3D printer can produce an orthosis with high dimensional accuracy [35]. In the customized FOs market, the cost for a pair of custom-made FOs is from 194 to 485 USD in Taiwan. The photosensitive polymer resins used were approximately 160 mL during printing, and they cost approximately 12 USD. Based on the cost of the podiatrist's time and business overheads, the cost for the plaster-cast method is from 20.90 to 37.11 USD [36]. The cost for the 3D scan is from 7.48 to 11.22 USD. The 3D scanner and SLA 3D printer cost 4810 USD and 1295 USD, respectively. Although the capital costs of 3D scanners are higher, the consumable costs for the traditional fabrication of FOs are higher. However, the use of a low-cost 3D scanner, such as the Microsoft Kinect system (Microsoft, Redmond, WA, USA), and a low-cost 3D printer could fabricate custom FOs similar to traditionally made FOs [37]. The method provides a solution to digital design and manufacture that potentially overcomes the limitation of conventional subtraction manufacturing. In addition, an increasing amount of free open-source software is available, such as the Meshmixer software that we used; clinical staff can use such software, as it does not require a high level of engineering skill.

Some limitations of the study should be considered. First, patient satisfaction was not assessed in this study. Moreover, the present study focused on the immediate effects of 3D-printed FOs in patients with knee OA and did not evaluate long-term responses. The effects on pain and sensations of comfort should be evaluated over a longer period in future works. Second, kung fu shoes were used as the standard shoes in this study. Kung fu shoes have a low-sided cloth upper part and a flat, hard, plastic sole. It remains unclear whether 3D-printed FOs would alter the biomechanical effects in different types of shoes.

5. Conclusions

This study demonstrated the potential for 3D printing technology in custom FO manufacture with rapid and cost-effective fabrication. The 3D-printed FOs did not affect the AEM but caused a decrease in the peak AIM, and the first and second peak KAMs by changing the COP path laterally. Although the decrease in the KFM from the use of 3D-printed FOs was nonsignificant, such FOs reduce knee joint loading in patients with knee OA. This study provides a new choice of conservative treatment for knee OA.

Author Contributions: Conceptualization, C.-S.C. and K.-W.L.; methodology, C.-S.C. and K.-W.L.; investigation, K.-W.L.; resources, S.-H.W. and Y.-T.S.; data curation, K.-W.L. and Y.-T.S.; writing—original draft preparation, K.-W.L.; writing—review and editing, C.-S.C. and L.-W.C.; supervision, C.-S.C. and L.-W.C. All authors have read and agreed to the published version of the manuscript.

Funding: This research was partly funded by a Grant (MOST 109-2622-E-010-003) from the Ministry of Science and Technology.

Institutional Review Board Statement: The study was conducted according to the guidelines of the Declaration of Helsinki, and approved by the Institutional Review Board of National Yang-Ming University (protocol code YM106118E, 31 March 2018).

Informed Consent Statement: Informed consent was obtained from all subjects involved in the study.

Data Availability Statement: The data presented in this study are available on request from the corresponding author.

Conflicts of Interest: The authors declare no conflict of interest.

References

1. Cross, M.; Smith, E.; Hoy, D.; Nolte, S.; Ackerman, I.; Fransen, M.; Bridgett, L.; Williams, S.; Guillemin, F.; Hill, C.L. The global burden of hip and knee osteoarthritis: Estimates from the global burden of disease 2010 study. *Ann. Rheum. Dis.* **2014**, *73*, 1323–1330. [CrossRef] [PubMed]
2. Tang, X.; Wang, S.; Zhan, S.; Niu, J.; Tao, K.; Zhang, Y.; Lin, J. The prevalence of symptomatic knee osteoarthritis in China: Results from the China health and retirement longitudinal study. *Arthritis Rheumatol.* **2016**, *68*, 648–653. [CrossRef]
3. Wise, B.L.; Niu, J.; Yang, M.; Lane, N.E.; Harvey, W.; Felson, D.T.; Hietpas, J.; Nevitt, M.; Sharma, L.; Torner, J. Patterns of compartment involvement in tibiofemoral osteoarthritis in men and women and in whites and African Americans. *Arthritis Care Res.* **2012**, *64*, 847–852. [CrossRef]
4. Hurwitz, D.E.; Sumner, D.R.; Andriacchi, T.P.; Sugar, D.A. Dynamic knee loads during gait predict proximal tibial bone distribution. *J. Biomech.* **1998**, *31*, 423–430. [CrossRef]
5. Zhao, D.; Banks, S.A.; Mitchell, K.H.; D'Lima, D.D.; Colwell Jr, C.W.; Fregly, B.J. Correlation between the knee adduction torque and medial contact force for a variety of gait patterns. *J. Orthop. Res.* **2007**, *25*, 789–797. [CrossRef] [PubMed]
6. Manal, K.; Gardinier, E.; Buchanan, T.S.; Snyder-Mackler, L. A more informed evaluation of medial compartment loading: The combined use of the knee adduction and flexor moments. *Osteoarthr. Cartil.* **2015**, *23*, 1107–1111. [CrossRef] [PubMed]
7. Chan, G.N.; Smith, A.W.; Kirtley, C.; Tsang, W.W. Changes in knee moments with contralateral versus ipsilateral cane usage in females with knee osteoarthritis. *Clin. Biomech.* **2005**, *20*, 396–404. [CrossRef]
8. Brandon, S.C.; Brown, M.J.; Clouthier, A.L.; Campbell, A.; Richards, J.D.; Deluzio, K.J. Contributions of muscles and external forces to medial knee load reduction due to osteoarthritis braces. *Knee* **2019**, *26*, 564–577. [CrossRef]
9. Shull, P.B.; Silder, A.; Shultz, R.; Dragoo, J.L.; Besier, T.F.; Delp, S.L.; Cutkosky, M.R. Six-week gait retraining program reduces knee adduction moment, reduces pain, and improves function for individuals with medial compartment knee osteoarthritis. *J. Orthop. Res.* **2013**, *31*, 1020–1025. [CrossRef] [PubMed]
10. Chapman, G.J.; Parkes, M.J.; Forsythe, L.; Felson, D.; Jones, R. Ankle motion influences the external knee adduction moment and may predict who will respond to lateral wedge insoles?: An ancillary analysis from the SILK trial. *Osteoarthr. Cartil.* **2015**, *23*, 1316–1322. [CrossRef] [PubMed]
11. Duivenvoorden, T.; van Raaij, T.M.; Horemans, H.L.; Brouwer, R.W.; Bos, P.K.; Bierma-Zeinstra, S.M.; Verhaar, J.A.; Reijman, M. Do laterally wedged insoles or valgus braces unload the medial compartment of the knee in patients with osteoarthritis? *Clin. Orthop. Relat. Res.* **2015**, *473*, 265–274. [CrossRef] [PubMed]
12. Jones, R.K.; Chapman, G.J.; Parkes, M.J.; Forsythe, L.; Felson, D.T. The effect of different types of insoles or shoe modifications on medial loading of the knee in persons with medial knee osteoarthritis: A randomised trial. *J. Orthop. Res.* **2015**, *33*, 1646–1654. [CrossRef]
13. Kakihana, W.; Akai, M.; Nakazawa, K.; Takashima, T.; Naito, K.; Torii, S. Effects of laterally wedged insoles on knee and subtalar joint moments. *Arch. Phys. Med. Rehabil.* **2005**, *86*, 1465–1471. [CrossRef] [PubMed]
14. Kakihana, W.; Torii, S.; Akai, M.; Nakazawa, K.; Fukano, M.; Naito, K. Effect of a lateral wedge on joint moments during gait in subjects with recurrent ankle sprain. *Am. J. Phys. Med. Rehabil.* **2005**, *84*, 858–864. [CrossRef]
15. Shimada, S.; Kobayashi, S.; Wada, M.; Uchida, K.; Sasaki, S.; Kawahara, H.; Yayama, T.; Kitade, I.; Kamei, K.; Kubota, M. Effects of disease severity on response to lateral wedged shoe insole for medial compartment knee osteoarthritis. *Arch. Phys. Med. Rehabil.* **2006**, *87*, 1436–1441. [CrossRef] [PubMed]
16. Hatfield, G.L.; Cochrane, C.K.; Takacs, J.; Krowchuk, N.M.; Chang, R.; Hinman, R.S.; Hunt, M.A. Knee and ankle biomechanics with lateral wedges with and without a custom arch support in those with medial knee osteoarthritis and flat feet. *J. Orthop. Res.* **2016**, *34*, 1597–1605. [CrossRef] [PubMed]
17. Hinman, R.S.; Bowles, K.A.; Metcalf, B.B.; Wrigley, T.V.; Bennell, K.L. Lateral wedge insoles for medial knee osteoarthritis: Effects on lower limb frontal plane biomechanics. *Clin. Biomech.* **2012**, *27*, 27–33. [CrossRef] [PubMed]
18. Chen, R.K.; Jin, Y.-A.; Wensman, J.; Shih, A. Additive manufacturing of custom orthoses and prostheses—A review. *Addit. Manuf.* **2016**, *12*, 77–89. [CrossRef]
19. Salles, A.S.; Gyi, D.E. An evaluation of personalised insoles developed using additive manufacturing. *J. Sports Sci.* **2013**, *31*, 442–450. [CrossRef]
20. Lin, K.-W.; Hu, C.-J.; Yang, W.-W.; Chou, L.-W.; Wei, S.-H.; Chen, C.-S.; Sun, P.-C. Biomechanical Evaluation and Strength Test of 3D-Printed Foot Orthoses. *Appl. Bionics. Biomech.* **2019**, *2019*, 4989534. [CrossRef]
21. Altman, R.; Asch, E.; Bloch, D.; Bole, G.; Borenstein, D.; Brandt, K.; Christy, W.; Cooke, T.; Greenwald, R.; Hochberg, M. Development of criteria for the classification and reporting of osteoarthritis: Classification of osteoarthritis of the knee. *Arthritis Rheum.* **1986**, *29*, 1039–1049. [CrossRef] [PubMed]
22. Forghany, S.; Nester, C.J.; Richards, B.; Hatton, A.L.; Liu, A. Rollover footwear affects lower limb biomechanics during walking. *Gait Posture* **2014**, *39*, 205–212. [CrossRef] [PubMed]
23. Hunt, M.A.; Birmingham, T.B.; Giffin, J.R.; Jenkyn, T.R. Associations among knee adduction moment, frontal plane ground reaction force, and lever arm during walking in patients with knee osteoarthritis. *J. Biomech.* **2006**, *39*, 2213–2220. [CrossRef] [PubMed]

24. Andriacchi, T.; Ogle, J.; Galante, J. Walking speed as a basis for normal and abnormal gait measurements. *J. Biomech.* **1977**, *10*, 261–268. [CrossRef]
25. Jones, R.K.; Zhang, M.; Laxton, P.; Findlow, A.H.; Liu, A. The biomechanical effects of a new design of lateral wedge insole on the knee and ankle during walking. *Hum. Mov. Sci.* **2013**, *32*, 596–604. [CrossRef] [PubMed]
26. Nakajima, K.; Kakihana, W.; Nakagawa, T.; Mitomi, H.; Hikita, A.; Suzuki, R.; Akai, M.; Iwaya, T.; Nakamura, K.; Fukui, N. Addition of an arch support improves the biomechanical effect of a laterally wedged insole. *Gait Posture* **2009**, *29*, 208–213. [CrossRef]
27. Nigg, B.M.; Stergiou, P.; Cole, G.; Stefanyshyn, D.; Mündermann, A.; Humble, N. Effect of shoe inserts on kinematics, center of pressure, and leg joint moments during running. *Med. Sci. Sports Exerc.* **2003**, *35*, 314–319. [CrossRef]
28. Trepczynski, A.; Kutzner, I.; Bergmann, G.; Taylor, W.R.; Heller, M.O. Modulation of the relationship between external knee adduction moments and medial joint contact forces across subjects and activities. *Arthritis Rheumatol.* **2014**, *66*, 1218–1227. [CrossRef]
29. Sharma, L.; Hurwitz, D.E.; Thonar, E.J.M.; Sum, J.A.; Lenz, M.E.; Dunlop, D.D.; Schnitzer, T.J.; Kirwan-Mellis, G.; Andriacchi, T.P. Knee adduction moment, serum hyaluronan level, and disease severity in medial tibiofemoral osteoarthritis. *Arthritis Rheum.* **1998**, *41*, 1233–1240. [CrossRef]
30. Thorp, L.E.; Sumner, D.R.; Wimmer, M.A.; Block, J.A. Relationship between pain and medial knee joint loading in mild radiographic knee osteoarthritis. *Arthritis Care Res.* **2007**, *57*, 1254–1260. [CrossRef] [PubMed]
31. Miyazaki, T.; Wada, M.; Kawahara, H.; Sato, M.; Baba, H.; Shimada, S. Dynamic load at baseline can predict radiographic disease progression in medial compartment knee osteoarthritis. *Ann. Rheum. Dis.* **2002**, *61*, 617–622. [CrossRef]
32. Maly, M.R.; Acker, S.M.; Totterman, S.; Tamez-Peña, J.; Stratford, P.W.; Callaghan, J.P.; Adachi, J.D.; Beattie, K.A. Knee adduction moment relates to medial femoral and tibial cartilage morphology in clinical knee osteoarthritis. *J. Biomech.* **2015**, *48*, 3495–3501. [CrossRef]
33. Sinclair, J.; Hebron, J.; Taylor, P.J. The test-retest reliability of knee joint center location techniques. *J. Appl. Biomech.* **2015**, *31*, 117–121. [CrossRef]
34. Chuter, V.; Payne, C.; Miller, K. Variability of neutral-position casting of the foot. *J. Am. Podiatr. Med. Assoc.* **2003**, *93*, 1–5. [CrossRef] [PubMed]
35. Schrank, E.S.; Stanhope, S.J. Dimensional accuracy of ankle-foot orthoses constructed by rapid customization and manufacturing framework. *J. Rehabil. Res. Dev.* **2011**, *48*, 31. [CrossRef] [PubMed]
36. Payne, C. Cost benefit comparison of plaster casts and optical scans of the foot for the manufacture of foot orthoses. *Aust J. Podiatr. Med.* **2007**, *41*, 29–31.
37. Dombroski, C.E.; Balsdon, M.E.; Froats, A. The use of a low cost 3D scanning and printing tool in the manufacture of custom-made foot orthoses: A preliminary study. *BMC Res. Notes* **2014**, *7*, 443. [CrossRef] [PubMed]